

# XFEM for fretting fatigue: straight VS mixed mode crack propagation

R. Hojjati-Talemi<sup>1</sup> and M. Abdel Wahab<sup>1</sup>

<sup>1</sup> Department of Mechanical Construction and Production, Faculty of Engineering and Architecture, Ghent University, 9000, Ghent, Belgium

[Reza.HojjatTalemi@UGent.be](mailto:Reza.HojjatTalemi@UGent.be)

**ABSTRACT.** *Fretting fatigue is a combination of two complex and serious mechanical phenomena, namely fretting and fatigue. The combination of these two phenomena can cause sudden fracture of components that are subjected to the oscillatory motions (fatigue) and at the same time are in contact with each other (fretting). Fretting fatigue lifetime can be divided to two different parts, namely crack initiation and crack propagation. In order to model fretting fatigue crack propagation, one of the simplifications that is widely used by researchers relies on the assumption of straight crack, normal to the contact surface.*

*In this study a modified fretting fatigue contact model in conjunction with eXtended Finite Element Method (XFEM) is used to monitor the effect of mode-mixity on fretting fatigue crack propagation. For this purpose, Python programming language along with ABAQUS<sup>®</sup> software is used to implement the application of XFEM to fretting fatigue crack propagation.*

## INTRODUCTION

Fretting occurs due to oscillatory relative displacement between two components that are in contact together, which results in damage at the contact interface. Once these components face cyclic fatigue load at the same time, fretting fatigue occurs. Fretting fatigue is a serious phenomenon, which leads to reduction of fatigue lifetime of component compared to pure fatigue case. The schematic view of experimental setup of fretting fatigue is illustrated in Fig. 1. In this setup two identical fretting pads are pushed against the fatigue specimen using constant load, which is called normal load and at the same time the specimen is subjected to oscillatory fatigue load. Then, at presence of these two non-proportional loads fretting fatigue fracture occurs.

Fretting fatigue failure process can be divided into two main portions, namely crack initiation and crack propagation. It is proven that in fretting fatigue failure scenario after nucleating crack at contact interface, in early stage of crack propagation its behavior is governed by frictional shear stress at the contact interface [1]. Afterwards, far from the contact the crack is dominated more by the axial bulk stress[1]. In terms of crack propagation, there are numerous studies [2-10] that have used fracture mechanics

approach to calculate fretting fatigue crack propagation lifetime. The fracture mechanics approach is based on calculating Stress Intensity Factors (SIFs) at the crack tip either in pre-cracked or un-cracked fatigue specimen. Rooke and Jones [2] used Green's function, which is purely analytical formula for calculating SIFs at the crack tip. Some authors used combination of Finite Element Analysis (FEA) methods and analytical formula such as Weight functions [4, 5, 8] to calculate SIFs for cracks normal to the contact line or having an arbitrary path inside the un-cracked fatigue specimen. Also, FEA method has been used widely to calculate SIFs at the crack tip in cracked specimen, more information can be found in references [3, 6, 7, 9, 11]. All of these studies have used the calculated SIFs at the crack tip using the assumption of Linear Elastic Fracture Mechanics (LEFM) to calculate the number of cycles of crack propagation from a certain crack length up to final failure. One of the major simplifications, which have been extensively used in FEA crack propagation models was based on using normal crack instead of mixed mode crack propagation. The reason that this assumption took into account was experimental observations that were reported in the literature, e.g. [12-14]. Furthermore, the hypothesis of normal crack can reduce the cost of numerical computation.

In this investigation the fretting fatigue crack propagation is modeled for both normal and mixed mode crack propagation in order to verify the validity of this assumption, especially at early stage of crack propagation. For this purpose, a modified fretting fatigue contact model in conjunction with eXtended Finite Element Method (XFEM) is introduced to study the behavior of fretting fatigue crack propagation. Python programming language along with ABAQUS<sup>®</sup> software was used to implement the application of XFEM. Finally, the fretting fatigue crack propagation of mixed mode crack is compared with the normal crack growth.

## **FRETTING FATIGUE MODIFIED CONTACT MODEL**

To solve the fretting fatigue contact model shown in Fig. 1, only half the specimen needs to be modeled using FEA because the experimental setup is ideally symmetric about the axial centerline of the specimen. As depicted in Fig. 2, the specimen was restricted from vertical movement along its bottom surface and free to roll in the  $x$ -direction along its bottom edge. The length of the specimen, width of the specimen and radius of pad were selected as  $L=20$  mm,  $b=10$  mm and  $R= 101.6$  mm, respectively. Both the fretting pad and the fatigue specimen had a unit depth. Both sides of cylindrical pad were restricted just to move in vertical direction. The Multi-Point Constraint (MPC) was also applied at the top of pad in order to avoid rotation due to the application of loads.

A two-dimensional, 4-node (bilinear), plane strain quadrilateral, reduced integration element (CPE4R) was used. The mesh size of  $5 \mu\text{m} \times 5 \mu\text{m}$  was considered at contact interface and decreased gradually far from the contact region for all models. This mesh size was gained by mesh convergence study which was achieved by previous study [15]. The contact between the fretting pad and the fatigue specimen was defined using the master-slave algorithm in ABAQUS<sup>®</sup> for contact between two surfaces. The circular

surface of the pad was defined as a slave surface and top surface of the specimen was defined as a master surface. Al 7075-T6 was selected for both the pad and the specimen with Modulus of Elasticity of 71 GPa and a Poisson's of 0.33. A Coefficient of Friction (COF) of 0.75 was used in this study. In all cases, the normal load and maximum axial stress were considered as  $F= 60$  N,  $\sigma_{axial} = 80$  MPa, respectively. Also, in order to study the effect of tangential load on crack propagation different ratios of  $Q/(\mu F) = 0.45, 0.67$  and  $0.9$  were used.

One of the challenging tasks in fretting fatigue is modeling the tangential load  $Q$  at contact interface. As shown in Fig. 1, the pads are restrained by springs so that a tangential fretting load  $Q$  is applied to the contact surface in phase with the axial bulk stress. In the modified model in this study, loads were applied in two steps. Normal contact load  $F$  was applied in the first step to establish contact between the fretting pad and the fatigue specimen. For applying tangential load  $Q$ , the experimental data was used. In experimental tests, the tangential force is defined by subtraction of the axial bulk load and the reaction load that can be measured by an attached load cell to the fixed side of specimen. Then, by dividing it by two, the tangential load at each side of specimen, which is in contact with fretting pad, is obtained as  $Q = \frac{(F_{axial} - F_r)}{2}$ , where  $F_{axial}$  is the axial bulk load and  $F_r$  is the axial reaction load. In order to model the effect of attached spring to the fretting pad for generating the tangential load, the reaction stress ( $\sigma_R$ ) can be calculated based on  $\sigma_R = Q/A_s - \sigma_{axial}$ , where  $A_s$  is cross section area of specimen as shown in Fig. 2: Therefore, in the modified model, in the second step, the maximum axial stress  $\sigma_{axial}$  and the reaction stress  $\sigma_R$  were applied at the same time at right and left sides of specimen, respectively, to match the experimental maximum cyclic loading condition. The accuracy of proposed model has been compared with the most of fretting fatigue FEA models that are available in literature by authors in [15].

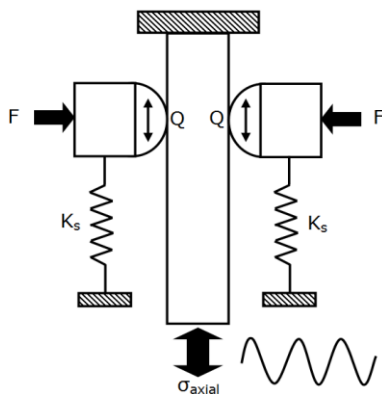


Figure 1. Schematic view of fretting fatigue experimental setup

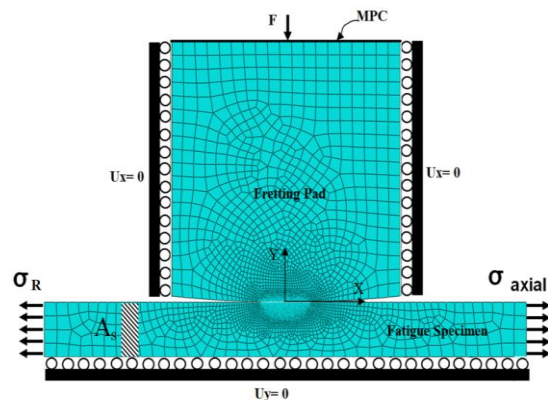
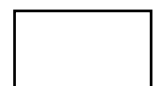


Figure 2. Modified FE model of fretting fatigue



## EXTENDED FINITE ELEMENT METHOD (XFEM)

Modeling stationary cracks using conventional finite element method needs the geometry of cracked body to be matched with the mesh. Then, in order to capture singularity at the crack tip, the mesh around the crack tip is needed to be considerably refined. Moreover, modeling crack propagation using mesh refinement techniques are really cumbersome, especially in 3-D and complex models. Recently, XFEM decreases inadequacy associated with re-meshing of the crack tip [16, 17]. The XFEM is the extended version of conventional FE method, which is based on concept of partition of unity method by Melenk and Babuska [18]. It allows local enrichment functions to be easily incorporated into a finite element approximation. For the purpose of fracture mechanics analysis, the enrichment functions typically consist of the near-tip asymptotic functions that capture the singularity around the crack tip and a discontinuous function that represents the jump in displacement across the crack line (in case of 2-D). The approximation for a displacement vector function  $\mathbf{u}^h(x)$  with the partition of unity enrichment is

$$\mathbf{u}^h(x) = \sum_{\forall I} N_I(x) \mathbf{u}_I + \sum_{j \in S_H} N_j(x) H(x) \mathbf{q}_j^0 + \sum_j \sum_{k \in S_c} N_k(x) F_j(x) \mathbf{q}_k^j, \quad (1)$$

Where,  $N_I(x)$  are the usual nodal shape functions for conventional finite element formulation. The first term on the right-hand side of Eq. 3,  $\mathbf{u}_I$ , is the usual nodal displacement vector associated with the continuous part of the finite element solution. The second term is the product of the nodal enriched degree of freedom vector,  $\mathbf{q}_j^0$ , and the associated discontinuous jump function  $H(x)$  across the crack line. The third term is the product of the nodal enriched degree of freedom vector,  $\mathbf{q}_k^j$ , and the related elastic asymptotic crack-tip functions,  $F_j(x)$ .

The usual nodal displacement vector,  $\mathbf{u}_I$ , is implemented to all the nodes in the FEA model. The second term, i.e.  $N_j(x)H(x)\mathbf{q}_j^0$ , is valid for nodes whose shape function support is cut by the crack. The third term,  $N_k(x)F_j(x)\mathbf{q}_k^j$ , is used only for nodes whose shape function support is cut by the crack tip.

Fig. 3 shows the discontinuous jump function across the crack line,  $H(x)$ , which is defined by:

$$H(x) = \begin{cases} 1 & \text{for } (\mathbf{x} - \mathbf{x}^*) \cdot \mathbf{n} \geq 0, \\ -1 & \text{else,} \end{cases} \quad (2)$$

Where  $\mathbf{x}$  is a sample integration (Gauss) point,  $\mathbf{x}^*$  is the point on the crack closest to  $\mathbf{x}$ , and  $\mathbf{n}$  is the unit outward normal to the crack at  $\mathbf{x}^*$ . Fig. 3 also depicts the asymptotic crack tip functions in an isotropic elastic material,  $F_1(r, \theta)$ , which are given by

$$\{F_1(r, \theta)\}_{l=1}^4 = \left\{ \sqrt{r} \cos\left(\frac{\theta}{2}\right), \sqrt{r} \sin\left(\frac{\theta}{2}\right), \sqrt{r} \sin\left(\frac{\theta}{2}\right), \sqrt{r} \cos\left(\frac{\theta}{2}\right) \sin(\theta) \right\}, \quad (3)$$

Where  $(r, \theta)$ , is a polar coordinate system with its origin at the crack tip and  $\theta = 0$  is tangent to the crack faces near the crack tip. These functions span the asymptotic crack-tip function of elasto-statics.

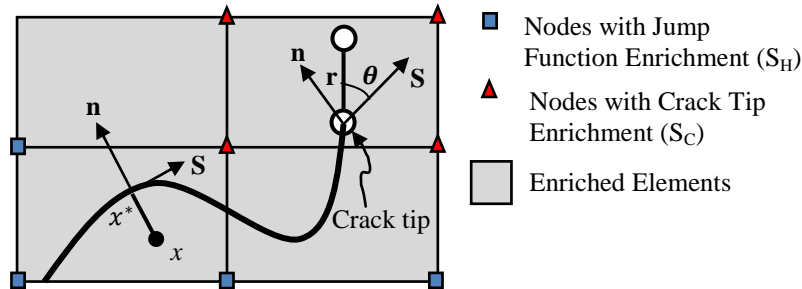


Figure 3. Normal and tangential coordinates for a smooth crack

There are a lot of studies which are aimed to impalement XFEM feature in conjunction with conventional FEA software. For instance, Giner *et al.* [7] have carried out a two-dimensional implementation of XFEM within the FE software ABAQUS by means of user subroutines. Since after ABAQUS 6.9<sup>®</sup>, the XFEM feature is added with some limitations by developers, in this study this capability was used to model the 2-D fretting fatigue crack propagation. One of the limitations that should be solved is extracting the SIFs at the crack tip for a 2-D stationary crack. This will be elaborated on later.

## FRETTING FATIGUE CRACK PROPAGATION

When applying fracture mechanics to fretting fatigue, three questions will arise, where is the location of initial crack? How long is it? And what is its initial orientation? To answer the first question, the stress distribution at the contact interface was monitored under linear elastic material behavior and data for initial length and orientation were extracted from literature [13, 19]. The location of the crack as it is proven by experimental observation [13, 19] is at or near to the trailing edge of contact which is the edge at side of applied bulk stress.

For fretting fatigue crack propagation model the crack inserted at  $x/a=1$ , where 'x' is the contact distant and 'a' is the semi contact width in the FE model configuration that is shown in Fig. 2. The crack propagation angle was chosen to be  $45^\circ$ , as it is mentioned, previous experimental studies available in literature have shown that the crack in fretting fatigue tests always initiated at or very near to the trailing edge with angle of  $\pm 45 \pm 15^\circ$ . Therefore, in the first step, an initial crack of length,  $l_0=50 \mu\text{m}$ , is introduced in the contact surface. Also, crack length increment of  $\Delta l=50 \mu\text{m}$  is considered for crack propagation. The loading and boundary conditions are the same as used for contact model. In this study, at each loading condition the crack propagation is modeled using normal and mixed mode crack propagation approach along with zero stress ratio.

### Calculating stress intensity factor

One of the main restrictions of ABAQUS's XFEM capability up to date (ABAQUS® 6.11) is that it is not possible to extract the SIFs for a 2-D stationary crack. After modeling cracked fatigue specimen based on the stress and displacement fields at the crack tip,  $J$  integral approach was used to calculate the SIFs for LFM assumption. The original form of the  $J$ -integral for a line contour surrounding the crack tip can be written as:

$$J = \oint_{\Gamma} W \, dy - \oint_{\Gamma} (t_x \frac{\partial u_x}{\partial x} + t_y \frac{\partial u_y}{\partial y}) \, ds, \quad (4)$$

In which,  $W = \sigma_{ij} d\varepsilon_{ij}$ , is the strain energy density ( $\sigma_{ij}$  and  $\varepsilon_{ij}$  as stress and strain tensors),  $t_x$  and  $t_y$  are the components of the traction vector which acts on the contour,  $u_x$  and  $u_y$  are the displacement components, and  $ds$  is a length increment along the contour  $\Gamma$ . Which in case of LFM the  $J$  is equal to energy release rate  $G$  ( $J = G = \frac{K_I^2}{E'}$ ), with  $E' = E/(1 - \nu^2)$  in plane strain problem. Finally the relation between mode I and mode II was calculated by using the local displacement fields  $u_n$  and  $u_t$  respectively, normal and tangent to the crack tip directions ( $q = \frac{u_t}{u_n} = \frac{K_{II}}{K_I}$ ). The maximum tangential stress criterion was used in order to calculate the propagation angel  $\theta_p$ . Based on stress field near the crack tip the direction of crack propagation was obtained using following equation:

$$\theta_p = \cos^{-1} \left( \frac{3K_{II}^2 + \sqrt{K_I^4 + 8K_I^2 K_{II}^2}}{K_I + 9K_{II}^2} \right), \quad (5)$$

## RESULTS AND DISCUSSION

In order to verify the contact model, two assumptions were taken into account. The first one was the elastic behavior of material, while the second was the Half Space assumption. Thus, the boundaries can be considered infinite if one half of the fretting specimen width,  $b$ , is equal to or greater than ten times the contact half width,  $a$ , or in other words  $b/a > 10$ . In this study, the analytical and FEA were  $a_{analytical} = 441 \, \mu\text{m}$  and  $a_{FEA} = 442 \, \mu\text{m}$ , respectively. Fig. 4. represents the correlation between FEA results and analytical solution [1] for the shear stress distribution at the contact interface. Furthermore, as expected the graph shows that with decreasing the tangential load from 40 N to 20 N, reverse slip occurs at contact edge.

Fig. 5 shows the relation between the calculated SIFs at the crack tip for mixed mode and normal crack propagation in case of  $Q = 40 \, \text{N}$ . As it can be seen from the figure, after 200  $\mu\text{m}$  crack length the assumption of normal crack works perfectly and can be used instead of mixed mode crack propagation. However, for small cracks for instance

50  $\mu\text{m}$  crack length there is 62% deviation between KI for normal and mixed mode crack. Moreover, it can be seen that after the crack length 0.5 mm the crack is governed by axial bulk stress and the extracted SIFs are yielding to results, which was calculated analytically for Double Edge Notch Tension (DENT) specimen form [20].

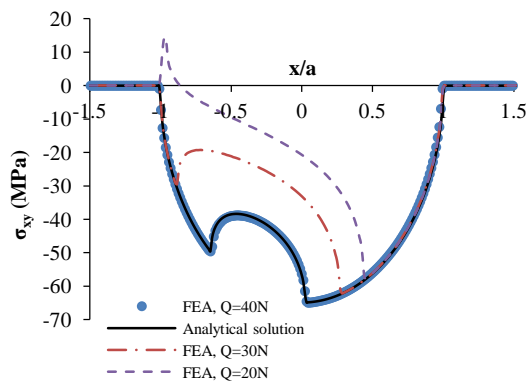


Figure 4. Validation of FEA model of fretting fatigue with analytical solution

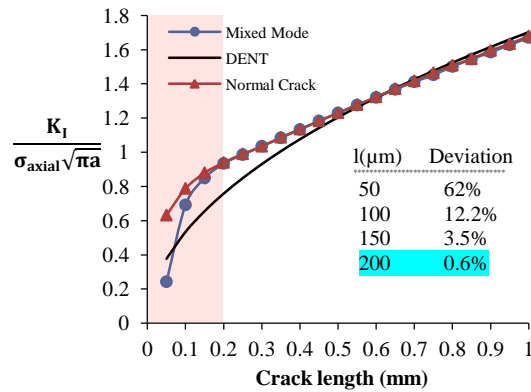


Figure 5. Distribution of normalized calculated SIFs VS crack length

Fig. 6 illustrates the effect of different tangential load at the contact interface on the calculated SIFs for cracks normal to the fatigue specimen surface and mixed mode crack propagation. The trend can be extended to all cases. From the crack length 200  $\mu\text{m}$ , the crack will be governed by axial stress, which is relatively far from contact region. Moreover, this graph shows the relation between tangential stress distributions inside the fatigue specimen at trailing edge of contact. It is interesting to note that with increasing the tangential load from 20 N to 40 N, the tangential stress also increases near contact interface and reaches a plateau far from contact area.

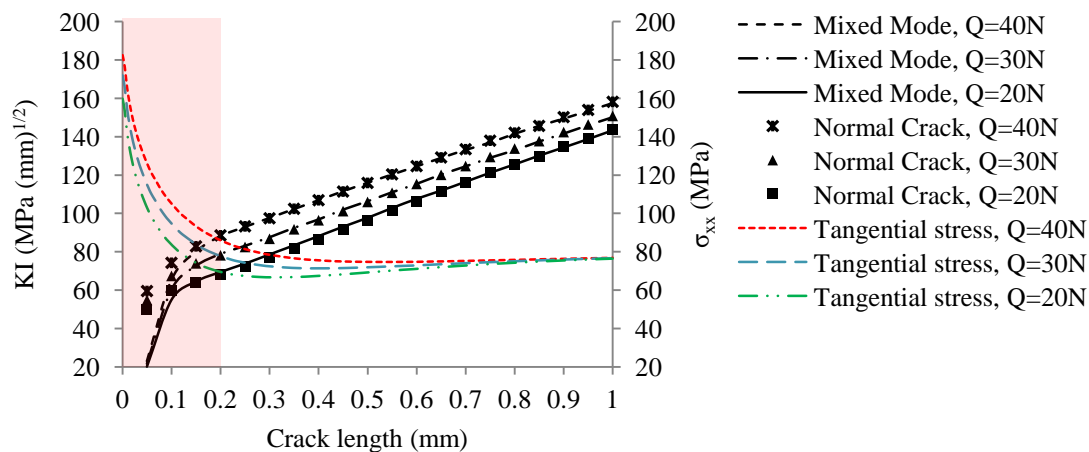


Figure 6. Comparison of SIFs and tangential stress ( $\sigma_{xx}$ ) for different tangential loads

## CONCLUSION

In this study, the effect of mode mixity crack propagation of fretting fatigue was investigated. The results showed clearly that at the onset of crack propagation, mixed mode crack propagation can have significant effect on the calculated SIFs, which are important parameters to calculate fretting fatigue crack propagation lifetime. Furthermore, it is worse to mention that after finding the transition crack length from mixed mode to mode I crack propagation the assumption of using normal crack is applicable. However, finding this certain crack length might be a challenging task.

## ACKNOWLEDGMENTS

The authors wish to thank the Ghent University for the financial support received by the Special Funding of Ghent University (Bijzonder Onderzoeksfonds), in the framework of BOF project (BOF 01N02410).

## REFERENCES

1. Hills, D.A., Nowell, D. (1994) *Mechanics of fretting fatigue*, Kluwer Academic Publishers, Dordrecht, Boston.
2. Rooke, D.P., Jones, D.A. (1979) *J. Strain Anal. Eng. Des.* **14**, 1-6.
3. Kondoh, K., Mutoh, Y. (2000). In: *Current Technology and Practices*, Hoepfner, D W., Chandrasekaran, V., C. B. Elliott (Eds), American society for Testing and Materials, West Conshohocken, PA,
4. Nicholas, T., Hutson, A., John, R., Olson, S. (2003) *Int. J. Fatigue*, **25**, 1069-1077.
5. Muñoz, S., Navarro, C., Domínguez, J. (2007) *Eng. Fract. Mech.* **74**, 2168-2186.
6. Giner, E., Tur, M., Vercher, A., Fuenmayor, F.J. (2009) *Tribol. Int.* **42**, 1269-1275.
7. Giner, E., Navarro, C., Sabsabi, M., Tur, M., Domínguez, J., Fuenmayor, F.J. (2011) *Int. J. Mech. Sci.* **53**, 217-225.
8. Navarro, C., Muñoz, S., Domínguez, J. (2011) *Strain*, **47**, e283-e291.
9. Sabsabi, M., Giner, E., Fuenmayor, F.J. (2011) *Int. J. Fatigue*, **33**, 811-822.
10. Hojjati-Talemi, R., AbdelWahab, M., De Baets, P. (2012) *Tribol. Trans.* In press.
11. Hojjati-Talemi, R., AbdelWahab, M., De Baets, P. (2011) *JPCS*, **305**, 12-61.
12. Ruiz, C., Boddington, P.H.B., Chen, K.C. (1984) *Exp. Mech.* **24**, 208-217.
13. Szolwinski, M.P., Farris, T.N. (1998) *Wear*, **221**, 24-36.
14. Navarro, C., Garcia, M., Dominguez, J. (2003) *Fract. Eng. Mater. Struct.* **26**, 459-468.
15. Hojjati-Talemi, R., Wahab, M.A., Pauw, J.D. (2012) *Proceeding of SCAD conference*, 207-220.
16. Moës, N., Dolbow, J., Belytschko, T. (1999) *Int. J. Numer. Methods Eng.* **46**, 131-150.
17. Belytschko, T., Black, T. (1999) *Int. J. Numer. Methods Eng.* **45**, 601-620.
18. Melenk, J.M., Babuška, I. (1996) *Comput. Meth. Appl. Mech. Eng.* **139**, 289-314.
19. Szolwinski, M.P., Farris, T.N. (1996) *Wear*, **198**, 93-107.
20. Mohammadi, S. (2008) *Extended finite element method*, Blackwell publishing Ltd.